The Eruption in Fagradalsfjall (2021, Iceland): How The Operational Monitoring and The Volcanic Hazard Assessment Contributed to Its Safe Access

Sara Barsotti (sara@vedur.is)
Icelandic Meteorological Office: Vedurstofa Islands https://orcid.org/0000-0001-5750-0872
Michelle Maree Parks
Icelandic Meteorological Office: Vedurstofa Islands
Melissa Anne Pfeffer
Icelandic Meteorological Office: Vedurstofa Islands
Bergrún Arna Óladóttir
Icelandic Meteorological Office: Vedurstofa Islands
Talfan Barnie
Icelandic Meteorological Office: Vedurstofa Islands
Manuel Marcelino Titos
Icelandic Meteorological Office: Vedurstofa Islands
Kristín Jónsdóttir
Icelandic Meteorological Office: Vedurstofa Islands
Gro BM Pedersen
University of Iceland: Haskoli Islands
Ásta Rut Hjartardóttir
University of Iceland: Haskoli Islands
Gerður Stefansdóttir
Icelandic Meteorological Office: Vedurstofa Islands
Thorsteinn Johannsson
Environment agency of Iceland
Þórður Arason
Icelandic Meteorological Office: Vedurstofa Islands
Magnús Tumi Gudmundsson
University of Iceland: Haskoli Islands
Björn Oddsson
Department of Civil Protection and Emergency Management
Ragnar H Þrastarson
Icelandic Meteorological Office: Vedurstofa Islands
Benedikt Gunnar Ófeigsson
Icelandic Meteorological Office: Vedurstofa Islands
Kristín Vogfjörd
Icelandic Meteorological Office: Vedurstofa Islands
Halldór Geirsson
University of Iceland: Haskoli Islands
Tryggvi Hjörvar
Icelandic Met Office: Vedurstofa Islands
Sibylle von Löwis
Icelandic Met Office: Vedurstofa Islands
Guðrun Nina Pedersen

Icelandic Meteorological Office: Vedurstofa Islands

Eysteinn Már Sigurðsson

Icelandic Meteorological Office: Vedurstofa Islands

Research Article

Keywords: Fagradalsfjall eruption, safe access, operational response, volcanic hazards, eruption monitoring

Posted Date: March 28th, 2022

DOI: https://doi.org/10.21203/rs.3.rs-1453832/v1

Version of Record: A version of this preprint was published at Natural Hazards on January 7th, 2023. See the published version at https://doi.org/10.1007/s11069-022-05798-7.

Abstract

After more than a year of unrest, a small effusive eruption commenced in Fagradalsfjall on 19 March 2021. The eruption lasted six months with multiple fissure openings characterizing the first six weeks. During the eruption lava and low-level gases propagated over the complex terrain: a hyaloclastite massif with mountain peaks up to about 350 m asl with valleys in the between. It is uninhabited, but easily accessible at about 30 km distance from the Reykjavík capital area. While the eruption was on-going, more than 356,000 accesses were counted. Monitoring the onset, the eruption in real-time, forecasting the transport of gas and emplacements of lava flows, and assessing the hazards were instrumental in maintaining safe access to the area. In addition to data accessibility and interpretation, managing this volcanic crisis was possible thanks to a strong collaboration between the scientific institutions and civil protection agencies. The eruption presented an opportunity to tune, test and validate a variety of numerical models for hazard assessment as well as to refine and improve the delivery of information to the public, community members and decision makers. The monitoring team worked long hours during both the pre- and syn-eruptive phases for a safe access to the eruption site and to provide a regular flow of information. This paper reviews the eruption and its associated hazards. It also provides an overview of the monitoring setup, the adopted numerical tools and communication materials made available for informing the general public of possible eruption scenarios and exclusion zones.

Introduction

There is on average an eruption every 3–5 years in Iceland (Gudmundsson et al., 2008). Prior to the 2021 Fagradalsfjall event, the last eruption occurred in 2014–2015 at Bárðarbunga volcano (Barsotti et al., 2020; Gudmundsson et al., 2016; Sigmundsson et al., 2015). As such, the timing of the Fagradalsfjall eruption was not surprising. It was however not expected that a volcanic system on the Reykjanes Peninsula would erupt, as no eruptions had occurred in the region for almost 800 years (Sæmundsson et al., 2020). The Reykjanes Peninsula is the on-shore continuation of the Mid-Atlantic Reykjanes ridge. The Peninsula comprises four main volcanic systems, from west to east: the Reykjanes, Svartsengi, Krýsuvík, and Brennisteinsfjöll. Each of these systems are characterized by numerous strike-slip and normal faults, eruptive fissures and post-glacial lava flows. Along the Peninsula an array of adjacent N-S aligned strike-slip faults to accommodate the shearing motion of the oblique Reykjanes rift (Clifton & Kattenhorn, 2006; Saemundsson, 1978). However, a fifth system, Fagradalsfjall, is also situated on the Peninsula. It is defined as an embryonic system as it has no associated geothermal activity and it is lacking a fissure swarm (Sæmundsson et al., 2020). For this reason, this system has sometimes been considered a part of the neighbouring Krýsuvík volcanic system (Einarsson, 2019). While earthquake activity is high on the Peninsula (e.g. Björnsson et al., 2020; Clifton & Kattenhorn, 2006; Einarsson, 1991), eruptive periods occur infrequently; at intervals of 800–1000 years (Sæmundsson et al., 2020). However, the eruptive periods may last from few decades to ~ 500 years, comprising intermittent eruptions (Sæmundsson et al., 2020). These eruptions are generally effusive, although minor ash has been produced. On the Peninsula, the Fagradalsfjall volcanic system appears to have been the least active during postglacial times. The last prior eruption occurred over 6000 years ago and the system also has fewer faults and eruptions than the other volcanic systems. It was not active during the last three volcanic episodes in the area, during which all the other volcanic systems became activated (Sæmundsson et al., 2020).

The Reykjanes Peninsula entered a period of volcano-tectonic unrest more than one year prior the eruption. Seismic and intrusive activity caused a clear geophysical signals a few weeks before the eruption, enabling the Icelandic Meteorological Office (IMO), together with colleagues at the University of Iceland (UI), Environment Agency of Iceland (EAI), the Iceland GeoSurvey (ÍSOR), the Icelandic Institute of Natural History and the Department of Civil Protection and Emergency Management of the National Commissioner of the Icelandic Police (CP) to prepare for a possible escalation of events.

Successful volcanic eruption management requires preparation, interpretation of monitoring data and effective communications (Lowenstern et al., 2022; Pallister et al., 2019). These elements can be challenging, especially if the volcano has not erupted in modern times and if the site rapidly becomes a popular touristic attraction (Gaudru, 2014). The capability to determine possible eruptive scenarios depends largely on the amount of available data, including access to detailed geological maps and information concerning previous eruptions and episodes of unrest. Things may become even more complicated when there is also uncertainty regarding the location of possible fissure and vent openings, which is the case for the Icelandic volcanic systems, where the eruption can originate from a fissure anywhere within an area that can be hundreds of kilometers long and tens of kilometers wide (Gudmundsson et al., 2008).

Throughout the period of the 2019–2021 volcanic unrest, the Fagradalsfjall volcanic system was categorised as a part of the Krýsuvík volcanic system. It was elevated to a yellow aviation color code on 24 February 2021, when an earthquake of magnitude M5.6 shook the Reykjanes Peninsula, and GNSS stations in the area began to show rapid deformation on a daily basis and marking the onset of a dyke intrusion within the Fagradalsfjall region (Sigmundsson et al., 2022). At this time the Scientific Advisory Board, a consortium of experts from Icelandic agencies, called upon by the CP and including those named above, was called to meet regularly with the main purpose of 1) understanding and interpreting the underlying processes and 2) identifying and ranking likelihood of possible scenarios. The most likely scenario, based on past eruptive activity and mapped volcanic products (Einarsson, 2019; Sæmundsson et al., 2020), was identified to be an effusive eruption with release of volcanic gases into the atmosphere. At this time the location(s) of potential fissure openings remained uncertain as the segmented dike continued to propagate to its final length of approximately 9 km (see Fig. 1). The preparatory work that followed focused on the area that was at that time affected by elevated seismicity and deformation. Lessons learnt from the Bárðarbunga eruption (Barsotti et al., 2020; Ilyinskaya et al., 2017; M. Pfeffer et al., 2018) provided, for example, a basis on how to implement a monitoring and forecasting system for a gas-rich event. The proximity of the active area to the Reykjavík capital city and the international airport emphasized the need for enhanced monitoring as it also facilitated access to the area.

From the start of the eruption on 19 March 2021 at 20:30 UTC, four main eruptive phases were identified based on different source locations, eruptive styles, fluxes and associated hazards. At the time of writing (March 2022) there has been no eruptive activity since 18 September 2021 and the eruption was officially declared over three months later (Icelandic Meteorological Office, 2022). This paper provides an overview of the course of the events, the short-term to real-time hazard assessments performed and the communication of these findings. The results also reveal how a safe access and protected viewpoints were guaranteed for hundreds of thousands of people who visited the eruption site.

Background activity and the unrest phase

Installation of seismometers at the Reykjanes peninsula started in the 1970s (Klein et al., 1977) and before that time, only a few seismometers were located in Iceland. Seismicity, mainly on strike-slip faults, has been consistently detected on the peninsula, although it occurs in episodes (Björnsson et al., 2020; Einarsson, 2008). GPS geodetic measurements in Reykjanes started in early 1990s (Sturkell et al., 1994, 2006) and they reveal that most of the plate-spreading deformation in Reykjanes is taking place in the southern and central part of the peninsula, whereas less deformation is detected in the northern part (Sigmundsson et al., 2020). A general subsidence has been detected along the peninsula (Árnadóttir et al., 2009) with local subsidence due to geothermal power plants and inflation events which were observed during the past decades (Geirsson et al., 2010; Hreinsdóttir et al., 2001; Keiding et al., 2010). The entire Peninsula is geodynamically very active. However, the level of seismic activity and deformation characterizing the unrest which led up to the 2021 Fagradalsfjall eruption had never been seen since the start of instrumental recordings in Iceland.

This intense seismicity and ground deformation was observed during a 14-month long period of volcano-tectonic unrest along the Reykjanes Peninsula suggesting that a large portion of the Peninsula had reactivated. This unrest phase preceded both the pre-eruptive dyke intrusion and the eventual eruption at Fagradalsfjall (Fig. 1). Increased seismicity was initially detected in December 2019 in the Fagradalsfjall region. A seismic swarm initially occurred between 15 to 20 December 2019, comprising about 500 earthquakes > M1. These earthquakes were located at depths between 3 and 7 km, with two apparent trends – one NS and the other EW. This seismicity was followed by about 2 months of quiescence but on 21 January 2020 activity re-commenced on the Peninsula, with a small cluster of earthquakes detected near Grindavík town (10 km southwest of the previous earthquakes). On 22 January the earthquake activity increased, with about 100 earthquakes 5 km west of Fagradalsfjall (three ≥ M3).

At the same time deformation was detected at two cGPS stations in this area and verified by interferometric analysis of Sentinel-1 satellite images. In addition, temporal seismic velocity changes were detected between January and July 2020 at Mt. Þorbjörn-Svartsengi, Iceland, using seismic ambient noise signifying crustal changes likely due to crack opening (Cubuk-Sabuncu et al., 2021). Geodetic modelling of these observations indicated that the observed deformation was due to a pressure increase within the shallow crust directly west of Mt. Þorbjörn within the Reykjanes-Svartsengi volcanic system (Fig. 1). The most likely scenario cause of the seismic and deformation changes was modeled to be the intrusion of a magmatic sill at a depth of about 4 km, corresponding to a volume change of ~ 3 million m^3. A plan for enhanced monitoring of the Reykjanes Peninsula was then implemented. Three additional cGPS instruments and one additional seismometer were installed in the area, data from the seismic

instruments operated by ÍSOR and CAS (Czech Academy of Sciences) were integrated into the IMO real-time processing and monitoring system and the frequency of gas measurements at high-temperature geothermal areas on the Reykjanes Peninsula including at Svartsengi, Eldvörp, Gunnuhver, and Seltún was increased.

The initial intrusion detected in January 2020 near Mt. Þorbjörn was followed by two additional sill-type intrusions at the same location. These were intruded between 6 March – 17 April, and 15 May – 22 July 2020. The three intrusions were located at similar depths at about 6–7 km, had similar geometries and comprised a total volume change of about 9 million m^3. In mid-July 2020 a fourth inflation event was detected on the Reykjanes Peninsula, this time in the Krýsuvík volcanic system to the East of Fagradalsfjall. This last episode lasted several weeks and geodetic inversion of both cGPS and InSAR observations indicated that the deformation was produced by a combination of a deflating sill-like source at a depth of ~ 16 km and inflation of a body at a depth of ~ 6 km by a volume change of about 5 million m^3.

During this period of intrusive activity (January 2020 – February 2021), seismicity switched on and off along various regions across the Peninsula, probably in relation to a combination of processes – intrusions, triggered seismicity and background activity of tectonic earthquakes. Almost 7000 earthquakes > M1 extending across a 40 km long segment between the westernmost tip of Reykjanes and Kleifarvatn were detected (see Fig. 1). By this time, it was evident that the reactivation of the Peninsula was most likely triggered by magma inflow at mid crustal depths.

The M5.6 earthquake that shook the Reykjanes Peninsula on 24 February 2021 at 10.05 UTC, marked a new chapter in activity with the onset of a dyke propagation in the vicinity of Fagradalsfjall. This was characterized by even more intense seismic swarms extending over a much larger area than seen before. During the first 24 hours ~ 1200 earthquakes > M1 (67 > M3) were automatically detected, not only in the region of emplacement but extending west to Svartsengi (along the plate boundary) and east to Krýsuvík geothermal area. This dyke was intruded over a period of three weeks and comprised multiple segments, with a total length of about 9 km, extending from south of Keilir to Lyngbrekkur (see Fig. 1). Geodetic inversions of GPS and InSAR observations indicated a total intruded volume of about 30 million m^3 (Sigmundsson et al., 2022) substantially larger than the previous intrusions.

Operational geophysical and atmospheric monitoring setup

A variety of sensors and instruments were installed to stream data to IMO, the Volcano Observatory in Iceland, to follow changes in activity (Figs. 1 and 2). In addition to these data streams, complementary monitoring resources were made available, through consolidated collaboration between the institutions involved in the eruption response, and included information/observations/data available at different temporal frequencies. Some acquisitions were done by regular streaming and others via campaign measurements.

- Streaming data:
    - Continuous real-time or near-real-time (NRT) surveillance provided by the seismic network, gas stations, web cameras, automatic weather stations, weather radars, ceilometers, lidars, ground-temperature probes and selected cGPS stations;
    - Several acquisitions per day provided by cameras, satellite products, MultiGAS and scanning DOAS, cGPS stations;
    - Several satellite synthetic aperture radar (SAR) acquisitions per week used for forming interferograms.
- Campaign activity:
    - Several acquisitions per week provided by DOAS traverses;
    - Sporadic tephra and rainwater collection, drone-borne and ground-based MultiGAS, FTIR, visual observations, lava sampling and surveillance flights for lava flow mapping;
    - Overflights;
    - Lava sampling.

Twenty-five cGPS stations were located within a 20 km radius of the eruption site and, together with twelve seismometers (within the same area), this was the backbone of the geophysical monitoring network operational at the Volcano Observatory (IMO). The data were streaming in real-time (or NRT) to the operation monitoring room where the natural hazards specialists on duty were following the evolution of the eruption 24/7. In the pre- and syn-eruption phases, satellite products (Sentinel-1, CSK) were regularly acquired (with a frequency of between 1 to 8 days for CSK, and every 6 days for Sentinel-1 in both ascending and descending passes) to detect ground deformation signals. The ground-based and satellite-borne deformation observations and seismic measurements were integrated via source modeling to determine the most likely source of the observed changes such as magmatic intrusions and co-eruptive subsidence due to magma removal.

When the eruption started, the primary monitoring needs were to observe the volcanic cloud and estimate its height and concentration of SO_2 for assessing and forecasting the potential impact of volcanic gas pollution at ground level in inhabited areas. At the same time, tracking the lava flows and estimating effusion rate was needed to anticipate the probable evolution of the lava field and the local hazard affecting those visiting the eruption site. Ground temperature probes, for continuous monitoring, were installed in cracks that had opened in the ground towards the northeast and southwest of the eruption site in the event fissures would continue to propagate endangering visitors.

DOAS (Differential Optical Absorption Spectrometer) is a UV remote sensing spectrometer that was used in both traverse and scanning modes to provide an estimate of SO_2 emitted at the source. A scanning DOAS was installed at about 10 km NNW of the eventual eruption site prior to the eruption onset and two ready-to-be-deployed scanning systems were prepared so they could be quickly installed after the eruption started (Fig. 1; 6 km to the NW and 4.5 km to the SW). A DOAS system for making car and plane traverses was also made ready.

Ground-based and drone-borne MultiGAS measurements were made sporadically when possible. MultiGAS measures the composition of the volcanic gases H_2O, CO_2, SO_2, H_2S (and H_2 for some measurements) in situ. One MultiGAS was installed after the onset of the eruption close to the first vent, on a hill that was initially assessed to be “safe”, in relation to current lava flows (Fig. 2). Unfortunately for the station, the fifth fissure opened up very close to this site and was subsequently destroyed.

A network of passive gas samplers was installed around Fagradalsfjall to assess air quality close to the eruption site (Fig. 2). Two different types of systems were installed, Crowcon systems that measure SO_2, H_2S and CO_2 and a home-built system based on Alphasense sensors that measure SO_2, O_2 and CO. Eventually, seven of these continuous gas monitoring systems were installed in a ring around the eruption site to account for most wind directions.

Prior to the eruption there was only one air quality monitoring station in the Reykjanes Peninsula measuring SO_2. It was located in Grindavík and operated be the energy company HS Orka to monitor possible pollution from the Svartsengi power plant north of the town. About three weeks before the onset of the eruption, the Environment Agency of Iceland (EAI) began installing more automatic monitoring stations. Five new SO_2 monitoring stations, with a resolution of a few $\mu g/m^3$ were installed in the urban areas closest to the eruption site (Fig. 1). Shortly after the eruption began, six monitoring stations were running in municipalities closest to the eruption site, with total population of about 25 000 inhabitants. The distance from the eruption site to these stations in nearby villages was from 9 km up to 18 km. Data from all these stations, as well as the near-eruption stations operated by IMO, were accessible on the open website airquality.is.

There are over ten automatic weather stations in the Reykjanes Peninsula, and during the eruption one station was added close to the eruption site. These stations provided valuable real-time information on weather and wind in the area, so people could plan a hiking route upwind from the main gas plume.

Since 2020, a ceilometer was operating in Hvassahraun, 17 km NNE of the eruption site and a scanning lidar plus a ceilometer have been permanently located at Keflavík airport since 2015 (see Fig. 1). A mobile lidar was initially located in Reykjavík with the purpose of detecting the potential volcanic aerosols when travelling toward or over the main capital area. However, on 1 July 2021 it was moved close to Grindavík to allow better coverage in the event the lava flowed to the sea. The fixed C-band weather radar at Keflavík airport 23 km to the NW, and a mobile X-band radar at Strandarheiði 13 km to the N were also in operation but due to the absence of volcanic ash in the atmosphere their data was of limited use.

Visible and thermal cameras were installed in different places to allow both far-field and close views of the eruption site and eruptive activity (Figs. 1 and 2), several of which were already installed before the eruption started. Some of the cameras were calibrated to provide quantitative information on height of volcanic plumes and lava fountains (Barnie et al., 2021), evolution of the lava field through a front tracking processing, changes in the crater's geometries and the detection of active vents. Eventually, cameras were installed to provide a clear view of the areas where the lava field was advancing towards important localities like walking paths and valley ridges.

Tephra and rain-water collection buckets were deployed at different distances from the eruption site to assess the amount of fallen material and the level of pollution in the precipitation. Pyroclasts formation was very minor and only occurred for a short period during the eruption.

The satellite thermal detection provided by MIROVA (Coppola et al., 2019, 2020) was regularly checked to monitor the level of activity and to keep track of the emission rates. Near real-time processing of Sentinel-5 products for SO_2 detection, provided a few images per day of long-range transport of the volcanic gas cloud and its magnitude.

Since the beginning of the eruption, photogrammetry of the lava field was acquired by aircraft. This information has been vital for assessing the lava effusion rates, extent and emplacement style (Pedersen et al., 2021), as well as to initialize the lava flow simulations to anticipate the possible further evolution of lava inundation.

The temporal evolution of the eruption

The eruption commenced relatively quietly on the evening of 19 March at about 20:30 UTC (https://en.vedur.is/about-imo/news/earthquake-swarm-in-reykjanes-peninsula) without any precursory escalation in either seismicity or deformation (Sigmundsson et al., 2022). The confirmation of its onset came from the people passing by the area and people from Grindavík, who phoned the IMO, as well as from the web cameras and satellite images. Lava initially erupted from a ~ 180 m long fissure which opened in a small valley, Geldingadalir in Fagradalsfjall (see Fig. 2) and that very quickly coalesced into two main adjacent craters. The lava started to pond in the valley and for almost two weeks no major changes affected the eruption scenario. Up to 6000 people visited the eruption site per day at the beginning of the eruption (Icelandic Tourism Dashboard, 2022), often forming crowded queues along the main walking paths and many staying in the surroundings of the lava field until evening waiting to take night-time photos (Fig. 3a and 3b).

During the initial phase, the eruption progressed with a fairly stable extrusion rate, on average 4.9 m^3/s lava (Pedersen et al., 2021), and 25–59 kg/s SO_2 (Pfeffer et al., in preparation). Seismicity was still elevated during this period and about one thousand earthquakes > M1 (manually checked) were detected in the vicinity of the eruption site during the first two weeks. This initial phase (Phase I) lasted until 5 April at 11:49 UTC (see Table 1), when two small new fissures opened about 600–800 m NE of the original one (and merged into one after less than one day). Phase II of the eruption was characterized by the opening of new fissures and lava extruding from these in variable amounts. Four additional fissures opened during the following eight days (Phase II-a; see Table 2) all aligned along the orientation of the initial dike intrusion (Sigmundsson et al., 2022, Hjartardöttir, in prep). On 14 April, amongst nine openings, seven were extruding lava, while gas and steam were release at all active vents (see Table 1 and Fig. 4). During Phase II-b of the eruption the activity alternated between different craters, some of which stopped issuing lava and others, which became more powerful. There were no differences in the gas composition measured at the different vents but there were different emission rates of SO_2 measured along the active fissures. The timeline of the activity from the different craters active during Phase II-b is summarized in Fig. 4 and Table 2. Web cameras show that after 27 April, lava production was coming from a single main vent (the fifth opening in temporal order, located at 63.8906°N, 22.2691°W) with variable lava outpouring (Phase III). Lava and gas were released through a fairly stable fountaining activity. Phase III-a lasted until 2 May, during which the lava fountains reached heights up to 350 m above sea level (about 120 m above vent) (Fig. 5a). The activity then changed (Phase III-b) and was characterized by a very intense pulsating activity. At this point, lava fountaining occurred at regular intervals separated by a few minutes. Since this pulsating style commenced, the top height of fountains reached maximum levels of about 430 m above sea level (about 200 m above vent), see Fig. 5a and 5b. Different gas compositions were measured by FTIR during and between lava fountaining events (Halldórsson et al., in review at Nature; Pfeffer et al., in preparation) and SO_2 concentrations directly above the vent were much higher during fountaining and very little between fountains (Halldórsson et al., in review at Nature; Pfeffer et al., in preparation). The

following phase (III-c) saw the alternation of lava fountains and intra-crater activity accompanied by sustained lava outpouring. The peak lava fountains reached almost 500 m above sea level. From the 28 June until the 18 September (Phase IV) the activity became less sustained and was characterized by pauses in activity in the crater for several hours (up to 35 hours consecutively in Phase IV-a and one week in Phase IV-b). During the pauses in activity, the SO_2 flux dropped to very low levels of few kg/s. In Phase IV-b the lava originated by a lateral upwelling region (~ 500 m SW of the main crater) which fed fast flows which were difficult to foresee and to reproduce by numerical models. Since 18 September no superficial activity has been identified and no new lava has been emitted from the crater.

Table 1
The table summarizes the four main phases (and related sub-phases) characterizing the eruptive activity in Fagradalsfjall, as described by different eruptive style and main associated hazards.

	Time-period	Eruptive style	Main associated hazards
PHASE I	19 March 2021–5 April 2021	Effusive eruption from one main fissure	Gas pollution, lava flows
PHASE II-a	5 April 2021–14 April 2021	Effusive eruption from (up to) eight fissures + opening of new fissures	Gas pollution, lava flows, opening of new fissures, fires
PHASE II-b	14 April 2021–27 April 2021	Effusive eruption from (up to) eight fissures	
PHASE III-a	27 April 2021–2 May 2021	Lava fountains from one main vent	
PHASE III-b	2 May 2021- 11 May 2021	Pulsating lava fountains from one main vent	Gas pollution, lava flows, opening of new fissures, bombs and tephra fallout
PHASE III-c	11 May 2021–28 June 2021	Outpouring of lava from the main crater, with occasional lava fountains and persistent intra-crater activity	Gas pollution, lava flows, opening of new fissures
PHASE IV-a	28 June 2021–2 September 2021	Intermittent activity in the crater with long (few hours up to 4 days) intervals	
PHASE IV-b	2 September 2021–18 September 2021	1 week-long repose followed 1 week-long activity	Sudden outbreak lava flows from upwelling area, gas pollution

Table 2
The timing of the openings that occurred in the first month of the eruption.

Eruptive openings	Opening date	Opening time (UTC)	Duration of the activity	Coordinates (degrees N, degrees W)
1a	2021-03-19	~ 20:30	Soon coalesced into 1b	63.8889,-22.2709
1b	2021-03-19	~ 20:30	~ 39 days	63.8892,-22.2706
2ab	2021-04-05	11:49	~ 12 days (the two openings coalesce into one source after ~ 1 day)	63.8952,-22.2637
3	2021-04-07	00:01	~ 20 days	63.8921,-22.2682
4	2021-04-10	03:13	~ 5 days	63.8934,-22.2662
5ab*c	2021-04-13	08:37 and 08:50	6 months	63.8910,-22.2689 63.8906,-22.2691 63.8905,-22.2685
6	2021-04-13	08:54	~ 15 days	63.8928,-22.2676

(*) The crater 5b is the one which kept erupting throughout the entire duration of the eruption.

Throughout the eruption and the different phases, a thick and dense plume was often visible, see Fig. 6a, which rose up to several kilometres due to buoyancy and inertial momentum. A time series overview of plume top and bottom height as measured from Hvassahraun camera (~ 12 km NE of the eruption site) is provided in Fig. 6b and shows a plume extending between a few hundred meters and 3000 m asl in the first month of the eruption. The month of May was characterized by an increasing plume height which ascended to 4100 m asl. This increase coincided with a change in meteorological conditions characterized by a stable atmosphere, with low wind speed (< 10 m/s) that persisted throughout a three-week period. The plume top height eventually decreased again staying below 2000 m for most of June and part of July. Around mid-August plume top heights again reached up to 3000 m asl. No good observations of the plume were acquired in September. For many weeks after the eruption ended, the rising heat from the lava field created a formidable plume during favourable meteorological conditions.

The associated hazards

The vicinity to populated areas as well as to the Keflavík international airport facilitated access of a large number of visitors to the eruption site since the first day of the eruption. Thousands of people per day were counted walking along a faintly marked path into an area, which initially was without any sort of infrastructure; including parking lots, secure paths or information signs. This presented a challenge for both the local rescue teams and the police who managed access to the area, as well as for Civil Protection who was in charge of the risk evaluation. Initially, access was allowed in most areas around the eruption site, however, with the progression of the events, changes were implemented to define a hazard zone where people were advised not to enter. The main hazards considered were the opening of new eruptive fissures, lava flows, gas pollution, spatters and tephra fall, and, to a lesser extent, dissolved constituents in waters.

Opening of new fissures

On 5 April the second eruptive fissure opened (also in a very silent manner) with no apparent warning observed by the monitoring network. The new opening was first observed by people visiting the eruption who watched it happening. The second opening occurred at about 600–800 m NE of the active crater and aligned along the main NE-SW direction of the mapped pre-eruptive dyke intrusion. Additional openings occurred on the 7, 10 and 13 April, and they were all located between the first two main fissures (see Fig. 3, Table 2). The seismic monitoring revealed that on many occasions, the tremor, as detected by several stations nearby the eruption site, showed a sharp decrease in intensity (2–4 Hz band) prior to the opening of new fissures. This was subsequently used as one of the criteria to alert the Civil Protection and those operating in the area to the potential of new openings. The possibility of

an eruptive opening with no warning was considered the highest risk for those visiting the area (both tourists, monitoring staff and scientists). This led to the installation of the continuous ground temperature instruments to possibly provide some warning prior to new crack openings. In addition, the implementation of real-time processing of cGPS data from stations closest to the active area was set up to anticipate the occurrence of new openings.

Lava flows

The eruption between the 19 March and 18 September was effusive, and as such lava flows were one of the main associated hazards. The area where the eruption took place is far from inhabited regions and no major infrastructure was directly exposed to lava invasion. Through regular aerial monitoring surveys and photogrammetry, it was possible to keep track of the lava field evolution and to assess the extrusion rate. The last survey confirmed that a total of $150 \pm 3 \times 10^6$ m^3 bulk volume of lava had been extruded over a six-month period and the lava field emplaced covers an area of 4.8 km^2 (Pedersen et al., 2021). Lava flows were issued from all fissures/openings, so that the lava propagated both toward the NE (Meradalir valley after 5 April) and towards the SE (Syðri-Meradalur valley after 14 April) after ponding for the first four weeks in the Geldingadalir valley. On 22 May the lava also started to flow down the Nátthagi valley through Syðri-Meradalir and on 13 June lava spilled from Geldingardalir over hiking trail A into Nátthagi, raising concern that lava might flow towards south-coast road and eventually enter the sea (see Fig. 2).

Cameras installed close to the eruption site (owned by IMO, the Icelandic Civil Protection and two TV channels) enabled the tracking of the lava fronts in different directions (see Fig. 2). The lava flow propagation was modelled using the MrLavaLoba numerical code (Tarquini et al., 2018; Vitturi & Tarquini, 2018) to anticipate the areas that might be inundated by lava, the most likely transport direction of active lava fronts and the potential timing of the filling of valleys and resulting spill over events. As additional fissures opened, and lava transport mechanisms kept changing it remained challenging to run the model to be able to reproduce the ongoing events and eruptive dynamics.

Gas pollution

The gas stations installed in communities and near the eruption site were essential to be able to advise communities about gas pollution. Based on the experience gained during the Bárðarbunga eruption (Gíslason et al., 2015; Pfeffer et al., 2018) station installation, data streaming, and communication and assessing the hazards due to potential pollution from the eruption was relatively smooth. A reference table correlating hazardous SO_2 concentration limits and suggested actions to take in case of exposure to such pollution was used, as during the eruption in 2014–2015 (https://ust.is/english/about-the-eai/responsibilities/air/air-pollution-during-a-volcanic-eruption/). Throughout the eruption, very few community stations in the Reykjanes Peninsula detected high levels of SO_2, with the highest concentrations recorded in Njarðvík on the 7 April (Fig. 7a). On that occasion the 10-minute concentration in air was up to 2000 $\mu g/m^3$ (Whitty et al., in preparation). The measurements at ground level were used for both warning people and to validate the forecast model. The stations in the vicinity of the eruption site, operated by IMO (see Fig. 2), were used to alert workers and visitors about dangerous levels of pollution in the area (Fig. 7b). The concentration of SO_2 often reached critical conditions near the eruption site, well beyond documented safe levels. The high concentrations varied both spatially and temporally and it was always possible for people to move away from the dense gas region to areas with safer concentrations.

In addition to the fresh plume transported directly from the eruption site to target areas, several cases of pollution due to a mature plume, richer in the oxidized sulfur species sulphate was detected. These events were interpreted to be an evolved eruption cloud where the SO_2 converted into SO_4^{2-} in the atmosphere (Carlsen et al., 2021; Ilyinskaya et al., 2017). An example is shown in Fig. 8 where the temporal evolution of SO_2, $PM_{2.5}$ and PM_1 concentrations are all plotted together for a station in Reykjavík (Bústaðavegur), 37 km NE of the eruption site, for the period 28 June – 7 July. The simultaneous presence of elevated concentration of fine particles (PM) and SO_2, detected on 2–3 July, indicates the presence of a mature volcanic cloud.

Spatters and tephra fall

Fresh lapilli fell in the area surrounding the eruption site (Fig. 9). A survey in the first two weeks of the eruption showed mm-sized pumices that travelled up to 600 m from the active vent with occasional cm-sized clasts observed. Pele's hair up to tens of cm were

observed up to 2 km distance from the vent. Initially the hazard impact due to the fallout of this material was assessed to be quite localized, but this changed when the activity became pulsating at the beginning of May (see Table 1).

The intense fountaining and the ensuing greater heights reached by pyroclasts, allowed the material to be launched further away from the main crater. 10-cm sized spatters and even larger were identified initially at a distance of 500 m from the crater and subsequently up to 1.5 km. Occasional strong winds facilitated the transport of very light and wide spatters of lava up to a distance of 1.7 km and it was not uncommon to be showered by lapilli rain if downwind of the eruption site. The hot spatter landing in dry moss sometimes caused short-lived fires. In light of this new hazard, collection buckets were set out around the eruption site for periodic collection, with the main aim of collecting tephra samples at different distances and to allow for proper assessment of pyroclast fallout and the implication for people on site.

Dissolved constituents in precipitation

More than 320 samples of precipitation were collected from 12 stations around the eruption, some close to the eruption site and some in the closest urban areas (Figs. 1 and 2). Twenty-nine samples were additionally taken from five lakes on the Reykjanes Peninsula. The precipitation and lake samples estimate environmental pressure, impact on groundwater and animals grazing in the vicinity of the eruption (~ 7.5 km). Analyses were made for pH and 48 elements (including F, Cl, SO_4, Si, Mg).

At the eruption site pH was constantly very low, on average 3.51, with the lowest measurement at 2.64 (estimated normal pH in precipitation is around 7). Concentration of all measured elements was elevated in most of the samples with the highest concentrations at the eruption site and at sites to the north of the eruption (see Fig. 1). Extreme peaks were measured in precipitation in two periods in late March (23–25 March) and early April (31 March– 05 April). In the first week of April, F concentration of 219.5 ppm was measured at the eruption site compared to 0.23 ppm in the lowest measured sample at this site. The second highest concentration was measured in the same location in late March and had value of 83.5 ppm. The average of all the samples for the summer period is about 14 ppm F, with an expected normal level of ~ 0.02 ppm. The other elements listed above show similar patterns.

Discussion

The eruption at Fagradalsfjall emitted a total amount of SO_2 on the order of 0.3–0.9 Mt (Pfeffer et al., in preparation) and a total bulk volume of lava of $150 \pm 3 \times 10^6$ m^3 (Pedersen et al., 2021). Although the 150 million m^3 bulk volume makes this eruption of average size for Iceland (Gudmundsson et al., 2008), it was small compared with the most recent basaltic eruption in Iceland, within the Bárðarbunga volcanic system in 2014–2015, when 9.2 Mt of SO_2 was released and 1.4 km^3 of lava was extruded (Pedersen et al., 2017; Pfeffer et al., 2018) during a similarly 6-month long eruptive period. However, the Fagradalsfjall eruption was distinctively hazardous, given its vicinity to inhabited areas and critical infrastructure, as well as the high number of visitors to the site, representing new challenges for both scientists and civil protection representatives. Its location between the International Airport of Keflavík and the Reykjavík Capital area, facilitated the access of numerous visitors to the eruption site. Holuhraun, in contrast, was an extremely remote location and access to the site was restricted during the 2014–2015 Bárðarbunga eruption. The Fagradalsfjall eruption therefore provides an excellent case study of a popular “touristic” eruption, which both individuals and tour companies came to visit. The former for experiencing the forces of nature, the latter for obvious economic interests (Donovan, 2018).

Based on the data from the Icelandic Tourist Board (2022) about 356 thousand people went to visit the eruption site during the period 24 March 2021–7 January 2022. During the first month of the eruption the number of visitors per day reached 6000 and was comprised of mainly local tourists. Since June, in correspondence to the border opening (following the COVID restriction release by the government), the tourism became more international. Despite the high number of visitors to the area, rough hiking trails and elevated SO_2 levels there were no fatalities.

Touristic eruptions require adequate monitoring and response, designed to support mitigation actions and decision-making procedures. Throughout the eruption, the goal was to provide a safe access route to the site, via regular and frequent (initially daily) meetings between the IMO’s surveillance room and its managers, selected scientists, the Civil Protection representatives, the police and rangers from the environmental institute that patrol the area on a daily basis. The latest observations, forecasts, and hazard assessment were communicated and discussed. Those attending the meeting had the chance to look at the scientific data and to

consider the implications for their actions in the field, like rerouting the walking paths, diverting people to more secure areas, and closing the area when needed because of very bad weather or expected very high concentration of gas at ground level.

Throughout the duration of the eruption, the types of associated hazards were changing along with variations in the eruptive style, reflecting a dynamic eruption which required a dynamic response. The hazards included: air pollution (both SO_2 and sulphates), acid precipitation, water and ground pollution, electrification of air, and, on a more local scale, ground fracturing, opening of new eruptive fissures, lava flows and lava spill over, tephra fallout and moss fires. Throughout the evolution of the eruption, the hazard assessment was also changing and needed to be adaptable to account for additional volcanic phenomena. However, different volcanic hazards had different temporal and spatial scales and for this reason different approaches were used for dealing with a local assessment and a proximal zone (within 50 km). No direct hazards were identified that posed a significant threat to the far-field, even though an occasional increase in SO_2 concentration was detected as far as Akureyri on 25 June (~ 280 km NE of the eruption site). In addition to the Reykjavík Capital area, where about 237,000 people live (Statistics in Iceland, 2022), there are several inhabited centers within a distance of 40 km from Fagradalsfjall: Keflavík and Njarðvík (19 600), Grindavík (3 500), Sandgerði (1 900), Garður (1 700), Vogar (1 300) and Hafnir (100). Resulting in a total over 264 000 persons, corresponding to about 72% of the entire population of Iceland, living next to the eruption and exposed directly to primary volcanic hazards.

As soon as the eruption started a forecasting system was implemented at the IMO with the purpose of informing people living on the Peninsula about the anticipated danger due to volcanic pollution. The CALPUFF dispersal code was reinstated (used during the Holuhraun eruption) to reproduce the SO_2 emission and transport from Fagradalsfjall (Barsotti et al., 2020; Scire et al., 2000). The two-days forecast ground concentration of SO_2 was available on IMO's web. The hourly forecast was shown using the color system used by the EAI (Directorate of Health, 2021) which follows the reference SO_2 thresholds. Two additional maps were provided that showed the most likely impacted areas within temporal windows of 6- and 24-hours. These maps had no specific reference to the intensity of the polluting event, but rather indicated where and when the volcanic cloud was expected to affect areas at the ground. These additional maps were introduced to deal with the expectation of a very detailed and precise forecast, that was actually very hard to obtain. Indeed, the closeness of the target locations to the eruption, the highly temporal variable plume height and the relatively low frequency of SO_2 flux estimates, reduced the capability of providing a reliable quantitative forecast (Barsotti, 2020). People were asked to check on the EAI website for the real-time measurement at the closest municipal station whenever the plume was forecasted to be near to them.

On a more local scale, the hazard assessment focused on dynamic phenomena that would have the potential to threaten people visiting the eruption site. The possibility of sudden fissure openings, high levels of volcanic gas, advancing lava fronts and lava outbreaks toward hiking paths, and occasional tephra fallout, all needed to be considered to ensure safe access. When the first "dangerous area" map was designed, the aim was to identify the area where additional openings were more likely to occur, based on the proximity to the modeled dyke intrusion at depth. This area was considered a high-danger region and people advised not to enter it. Subsequent hazard maps accounted for the extension of the lava field (as reconstructed mainly via aerial photogrammetry) by adding an extra buffer zone of about 100 m and was intended to prevent people from being subject to sudden lava outbreaks and exposure to fluid lava and high temperatures. The lava flow model results were not included into such maps as their temporal uncertainty was too large and the maps would have been prone to public misunderstanding. A very basic numerical tool was used to draw the areas anticipated to be affected by ejected lava spatters. The on-line ballistic trajectory tool developed by Mastin (2001) was adopted to identify preliminary contours of the hazard area effected by volcanic clasts fallout. Both calm and high-wind conditions were considered, as the wind in the Fagradalsfjall area could reach very high speeds (through the eruption duration the strongest measured wind was 34 m/s on the 12 May, and with wind gusts up to 48 m/s). The density of the volcanic pyroclasts was so low (roughly 500 g/m^3) that they were transported much further in the presence than absence of wind. Two circles of 500 m and 650 m radii were eventually added to the map, identifying the area where people were advised that in given conditions such fallout might occur, see Fig. 10. This area was primarily used by the air-traffic controller for helicopters to advise on where they might land when bringing people to the eruption. The hazard map (Fig. 10) was formally published on-line by the Icelandic Meteorological Office on 4 May 2021 and endorsed by the Civil Protection which passed it through key dissemination channels like Safe Travel (safetravel.is).

As the forecast of gas pollution over such a small area would have required a very precise numerical model and high-resolution meteorological data that were not available, the decision was taken to not attempt to model it, but to inform people that pollution

due to volcanic gas was expected anywhere surrounding the eruption site and they were asked to check the daily written forecast prepared by the weather forecaster on-duty, available on IMO's website, as well as directing them to the real-time data streaming from the stations installed at the eruption site which was available on EAI's website. In the first weeks of the eruption, when the rescue team volunteers detected elevated gas concentrations with their hand-held sensors, they would instruct people to leave the area and move up wind and to elevated places to avoid direct exposure. Advice from the CP was given to not bring young babies or pets to the eruption site. The level of pollution of surficial water was regularly reported to civil protection and recommendations were given to discourage to bring dogs or horses who might drink polluted water puddles.

Mitigation actions and coordinated response, as those listed above, guaranteed a protected visit to the eruption site for most people. However, it is also important to mention those occasions when support and intervention was required by local rescue teams. This included search and rescue for people lost during bad weather (mainly in the beginning of the eruption). Three people needed to be rescued by helicopter and several have been collected after being trapped by lava flows; more than 30 people asked for help because of exhaustion and/or hypothermia, and possibly gas poisoning (up to 30 people visited the Poison center at the Hospital for checks); 25 people suffered fractures and more than 30 needed assistance for other types of injuries (Landsbjörg, personal communication).

A completely new scenario was anticipated in the event of the lava flow advancing down Nátthagi valley and towards the sea on the south coast as no other natural obstacles would prevent the lava reaching the coastline within the remaining 1.5 km long distance. Eventually, the lava did not fill Nátthagi, but preparations for this possibility started as soon as the lava progressed further into the valley. The lava flow model, initialized for a short-term forecasting scenario, identified the most likely entry point into the sea (Fig. 11).

In Iceland, lava flow last entered the sea during the Heimaey eruption in 1973. This would trigger additional hazards to take into consideration. Amongst others the most relevant hazards considered were:

1) the production and release into the atmosphere of abundant HCl;

2) the potential for phreato-magmatic activity and the consequent production of ash in the atmosphere.

The recent experiences and lessons learnt during eruptions in Hawai'i from 2018 onwards, were initially considered to start designing the necessary instrumentation setup to monitor the air-quality aspects (Kullman et al., 1994; Mason et al., 2021). A preliminary plan discussed and agreed with representatives at the EAI included:

- Installation of HCl sensors for real time monitoring nearby the entry point as well as in the closest inhabited town of Grindavík;
- Regular filter-pack acquisitions to measure Cl, Fl and S compounds and heavy metals;
- Installation of Optical Particle Counters nearby the entry point and in Grindavík to assess the intensity of polluting events.

The mobile-lidar was moved to the Hópsnes Peninsula by Grindavík (Fig. 1) and the co-located calibrated camera was set pointing toward the likely entry point. The initial plan was that the camera would be used in assessing the plume height and enable a rapid mass eruption rate estimate and the initialization of ash dispersal numerical models. Indeed, the vicinity of the airport required a quick response in the event of the production of ash and tephra. The plan, agreed together with the air navigation service provider ISAVIA, was to immediately change the aviation color code to red if the lava began flowing into the sea, along with an initial SIGMET (SIGnificant METeorological information) (Barsotti et al., 2020) to be issued identifying the most likely area affected by ash contamination. A re-assessment would be done as soon as additional data became available to understand the severity and the intensity of the explosive component.

Conclusion

At the time of writing (March 2022), eruptive activity at Fagradalsfjall has ceased, following a 6-month long eruptive period characterized primarily by multiple fissure and vent openings, lava extrusion, lava fountaining and gas emissions. Elevated seismic activity and deformation changes continue in the region (confirmed by InSAR and GNSS) following the end of eruptive activity on 18 September. A second dike intrusion occurred at Fagradalsfjall between the 21–28 December 2021, following recharging of a deep reservoir that fed the 2021 eruption, although this did not culminate in an eruption. The future of this unrest is currently difficult to

foresee but may comprise multiple additional dike intrusions over the coming years, which may or may not culminate in eruptions. The activity at Fagradalsfjall has proven to be an invaluable opportunity to investigate and learn more about pre-eruptive monitoring, data interpretation, fissure eruption dynamics, low-level volcanic gases dispersal processes, lava flow simulation, volcanic hazard assessment and communication.

Its location and its easy access made this eruption very touristic with more than 356 thousand visitors in total since March 2021. Managing the accessibility to the site required strong collaboration between scientists and civil protection authorities. It has always been an Icelandic cultural priority that natural phenomena, even when potentially dangerous, should be safely enjoyed by people. Regular meetings between scientists and those in charge of operations, sharing of scientific data and numerical model results and an open dialogue have been essential ingredients for managing health and safety issues deeply related to volcano tourism.

This paper also reveals how important it is to define scenarios (based on monitoring data and/or numerical model results) for advanced preparation of monitoring setup, monitoring strategies and identification of hazards.

Declarations

Competing interests

The author(s) declare no competing interests.

References

1. Árnadóttir, T., Lund, B., Jiang, W., Geirsson, H., Björnsson, H., Einarsson, P., & Sigurdsson, T. (2009). Glacial rebound and plate spreading: Results from the first countrywide GPS observations in Iceland. *Geophysical Journal International*, *177*(2), 691–716.
2. Barnie, Talfan, Sigurðsson, Tryggvi, Pfeffer, Melissa, Arason, Þorður, & Barsotti, Sara. (2021, April 19). *A calibrated visual web camera network for measuring volcanic plume heights: Technical aspects and implementation for operational use*. European Geophysical Union. https://doi.org/10.5194/egusphere-egu21-15235
3. Barsotti, S. (2020). Probabilistic hazard maps for operational use: The case of SO 2 air pollution during the Holuhraun eruption (Bárðarbunga, Iceland) in 2014–2015. *Bulletin of Volcanology*, *82*(7), 1–15.
4. Barsotti, S., Oddsson, B., Gudmundsson, M. T., Pfeffer, M. A., Parks, M. M., Ófeigsson, B. G., Sigmundsson, F., Reynisson, V., Jónsdóttir, K., Roberts, M. J., Heiðarsson, E. P., Jónasdóttir, E. B., Einarsson, P., Jóhannsson, T., Gylfason, Á. G., & Vogfjörd, K. (2020). Operational response and hazards assessment during the 2014–2015 volcanic crisis at Bárðarbunga volcano and associated eruption at Holuhraun, Iceland. *Journal of Volcanology and Geothermal Research*, *390*, 106753. https://doi.org/10.1016/j.jvolgeores.2019.106753
5. Björnsson, S., Einarsson, P., Tulinius, H., & Hjartardóttir, Á. R. (2020). Seismicity of the Reykjanes Peninsula 1971–1976. *Journal of Volcanology and Geothermal Research*, *391*, 106369.
6. Carlsen, H. K., Ilyinskaya, E., Baxter, P. J., Schmidt, A., Thorsteinsson, T., Pfeffer, M. A., Barsotti, S., Dominici, F., Finnbjornsdottir, R. G., & Jóhannsson, T. (2021). Increased respiratory morbidity associated with exposure to a mature volcanic plume from a large Icelandic fissure eruption. *Nature Communications*, *12*(1), 1–12.
7. Clifton, A. E., & Kattenhorn, S. A. (2006). Structural architecture of a highly oblique divergent plate boundary segment. *Tectonophysics*, *419*(1–4), 27–40.
8. Coppola, D., Barsotti, S., Cigolini, C., Laiolo, M., Pfeffer, M., & Ripepe, M. (2019). *Monitoring the time-averaged discharge rates, volumes and emplacement style of large lava flows by using MIROVA system: The case of the 2014-2015 eruption at Holuhraun (Iceland)*.
9. Coppola, D., Laiolo, M., Cigolini, C., Massimetti, F., Delle Donne, D., Ripepe, M., Arias, H., Barsotti, S., Parra, C. B., & Centeno, R. G. (2020). Thermal remote sensing for global volcano monitoring: Experiences from the MIROVA system. *Frontiers in Earth Science*, *7*, 362.
10. Cubuk-Sabuncu, Y., Jónsdóttir, K., Caudron, C., Lecocq, T., Parks, M. M., Geirsson, H., & Mordret, A. (2021). Temporal Seismic Velocity Changes During the 2020 Rapid Inflation at Mt. Þorbjörn-Svartsengi, Iceland, Using Seismic Ambient Noise. *Geophysical Research Letters*, *48*(11), e2020GL092265.

11. Directorate of Health. (2021). *HEALTH RISKS DUE TO AIR POLLUTION FROM VOLCANIC ERUPTIONS - Guidelines for the public*. https://www.landlaeknir.is/servlet/file/store93/item45005/Haetta%20a%20heilsutjoni%20vegna%20loftmengunar_EN%202.pdf
12. Donovan, A. (2018). Sublime encounters: Commodifying the experience of the geos. *Geo: Geography and Environment*, *5*(2), e00067.
13. Einarsson, P. (1991). Earthquakes and present-day tectonism in Iceland. *Tectonophysics*, *189*(1–4), 261–279.
14. Einarsson, P. (2008). Plate boundaries, rifts and transforms in Iceland. *Jökull*, *58*(12), 35–58.
15. Einarsson, S. (2019). *Krýsuvík. In: Retrieved from*. Oladottir, B., Larsen, G. & Guðmundsson, M. T. Catalogue of Icelandic Volcanoes. IMO, UI and CPD-NCIP. http://icelandicvolcanoes.is/?volcano=KRY
16. Gaudru, H. (2014). Volcano tourism: The effect of eruptions and disasters. In *Volcanic tourist destinations* (pp. 337–350). Springer.
17. Geirsson, H., Árnadóttir, T., Hreinsdóttir, S., Decriem, J., LaFemina, P. C., Jónsson, S., Bennett, R. A., Metzger, S., Holland, A., & Sturkell, E. (2010). Overview of results from continuous GPS observations in Iceland from 1995 to 2010. *Jökull*, *60*, 3–22.
18. Gíslason, S. R., Stefánsdóttir, G., Pfeffer, M. A., Barsotti, S., Jóhannsson, Th., Galeczka, I., Bali, E., Sigmarsson, O., Stefánsson, A., Keller, N. S., Sigurdsson, Á., Bergsson, B., Galle, B., Jacobo, V. C., Arellano, S., Aiuppa, A., Jónasdóttir, E. B., Eiríksdóttir, E. S., Jakobsson, S., … Gudmundsson, M. T. (2015). Environmental pressure from the 2014–15 eruption of Bárðarbunga volcano, Iceland. *Geochemical Perspectives Letters*, *1*(0), 84–93. https://doi.org/10.7185/geochemlet.1509
19. Gudmundsson, M. T., Jónsdóttir, K., Hooper, A., Holohan, E. P., Halldórsson, S. A., Ófeigsson, B. G., Cesca, S., Vogfjörd, K. S., Sigmundsson, F., & Högnadóttir, T. (2016). Gradual caldera collapse at Bárdarbunga volcano, Iceland, regulated by lateral magma outflow. *Science*, *353*(6296), aaf8988.
20. Gudmundsson, M. T., Larsen, G., Höskuldsson, Á., & Gylfason, Á. G. (2008). Volcanic hazards in Iceland. *Jökull*, *58*, 251–268.
21. Halldórsson, S. A., Marshall, E., Caracciolo, E., Matthew, S., Bali, E., Rasmussen, M., Ranta, E., Gunnarsson, J., Guðfinnsson, G., Sigmarsson, O., Maclennan, J., Jackson, M., Whitehouse, M., Jeon, H., van der Meer, Q., Mibei, G., Kalliokoski, M., Repczynska, M., Rúnarsdóttir, R., … Stefánsson, A. (in review at Nature). *Rapid source shifting of a deep magmatic system revealed by the Fagradalsfjall eruption, Iceland*.
22. Hreinsdóttir, S., Einarsson, P., & Sigmundsson, F. (2001). Crustal deformation at the oblique spreading Reykjanes Peninsula, SW Iceland: GPS measurements from 1993 to 1998. *Journal of Geophysical Research: Solid Earth*, *106*(B7), 13803–13816.
23. Icelandic Meteorological Office. (2022). *Ekkert hraunflæði í þrjá mánuði við Fagradalsfjall*. https://www.vedur.is/um-vi/frettir/ekkert-hraunflaedi-i-thrja-manudi-vid-fagradalsfjall
24. Icelandic Tourism Dashboard. (2022). *Number of tourists at Geldingadalir eruption*. https://www.maelabordferdathjonustunnar.is/en/volcanic-eruption-in-geldingadalir
25. Ilyinskaya, E., Schmidt, A., Mather, T. A., Pope, F. D., Witham, C., Baxter, P., Jóhannsson, T., Pfeffer, M., Barsotti, S., & Singh, A. (2017). Understanding the environmental impacts of large fissure eruptions: Aerosol and gas emissions from the 2014–2015 Holuhraun eruption (Iceland). *Earth and Planetary Science Letters*, *472*, 309–322.
26. Keiding, M., Árnadóttir, T., Jónsson, S., Decriem, J., & Hooper, A. (2010). Plate boundary deformation and man-made subsidence around geothermal fields on the Reykjanes Peninsula, Iceland. *Journal of Volcanology and Geothermal Research*, *194*(4), 139–149.
27. Klein, F. W., Einarsson, P., & Wyss, M. (1977). The Reykjanes Peninsula, Iceland, earthquake swarm of September 1972 and its tectonic significance. *Journal of Geophysical Research*, *82*(5), 865–888.
28. Kullman, G. J., Jones, W. G., Cornwell, R. J., & Parker, J. E. (1994). Characterization of air contaminants formed by the interaction of lava and sea water. *Environmental Health Perspectives*, *102*(5), 478–482.
29. Lowenstern, J., Wallace, K., Barsotti, S., Sandri, L., Stovall, W., Bernard, B., Privitera, E., Komorowski, J.-C., Fournier, N., & Balagizi, C. (2022). Guidelines for volcano-observatory operations during crises: Recommendations from the 2019 volcano observatory best practices meeting. *Journal of Applied Volcanology*, *11*(1), 1–24.
30. Mason, E., Wieser, P. E., Liu, E. J., Edmonds, M., Ilyinskaya, E., Whitty, R. C., Mather, T. A., Elias, T., Nadeau, P. A., & Wilkes, T. C. (2021). Volatile metal emissions from volcanic degassing and lava–seawater interactions at Kīlauea Volcano, Hawai'i. *Communications Earth & Environment*, *2*(1), 1–16.

31. Mastin, L. G. (2001). *A simple calculator of ballistic trajectories for blocks ejected during volcanic eruptions*. US Department of the Interior, US Geological Survey.
32. Pallister, J., Papale, P., Eichelberger, J., Newhall, C., Mandeville, C., Nakada, S., Marzocchi, W., Loughlin, S., Jolly, G., & Ewert, J. (2019). Volcano observatory best practices (VOBP) workshops-a summary of findings and best-practice recommendations. *Journal of Applied Volcanology*, *8*(1), 2.
33. Pedersen, G. B. M., Gudmundsson, M. T., Óskarsson, Birgir, Belart, Joacquin, Gies, Nils, Hognadottir, Thordis, Hjartadottir, Ásta, Durig, Tobias, Reynolds, Hanna, Valsson, Guðmundur, Hamilton, Christopher, Gunnarsson, Andri, Pinel, Virginie, Berthier, Etienne, Einarsson, Pall, & Oddsson, Björn. (2021, December). *Volume, Discharge Rate and Lava Transport at the Fagradalsfjall Eruption 2021: Results from Near-Real Time Photogrammetric Monitoring*. American Geophysical Union, New Orleans. https://agu.confex.com/agu/fm21/meetingapp.cgi/Paper/935003
34. Pedersen, G., Höskuldsson, A., Dürig, T., Thordarson, T., Jonsdottir, I., Riishuus, M. S., Óskarsson, B. V., Dumont, S., Magnússon, E., & Gudmundsson, M. T. (2017). Lava field evolution and emplacement dynamics of the 2014–2015 basaltic fissure eruption at Holuhraun, Iceland. *Journal of Volcanology and Geothermal Research*, *340*, 155–169.
35. Pfeffer, M. A., Aiuppa, A., Scott, S., Stefánsson, Kjartansdóttir, R., Oppenheimer, C., Edwards, B., Hjörvar, T., Bitetto, M., & Giudice, G. (In preparation). *Ground-based gas measurements of the 2021 Fagradalsfjall eruption cloud*.
36. Pfeffer, M. A., Arellano, S., Petersen, G. N., Barnie, T., Barsotti, S., Bali, E., Hjörvar, T., Gudmundsson, G., & Vogfjörd, K. (In preparation). *SO2 emissions during the 2021 eruption of Fagradalsfjall, Iceland*.
37. Pfeffer, M., Bergsson, B., Barsotti, S., Stefánsdóttir, G., Galle, B., Arellano, S., Conde, V., Donovan, A., Ilyinskaya, E., & Burton, M. (2018). Ground-Based Measurements of the 2014–2015 Holuhraun Volcanic Cloud (Iceland). *Geosciences*, *8*(1), 29.
38. Saemundsson, K. (1978). Fissure swarms and central volcanoes of the neovolcanic zones of Iceland in Crustal evolution in northern Britain and adjacent regions. *Geological Journal Liverpool*, *10*, 415–432.
39. Sæmundsson, K., Sigurgeirsson, M. Á., & Friðleifsson, G. Ó. (2020). Geology and structure of the Reykjanes volcanic system, Iceland. *Journal of Volcanology and Geothermal Research*, *391*, 106501.
40. Scire, J. S., Strimaitis, D. G., & Yamartino, R. J. (2000). A user's guide for the CALPUFF dispersion model. *Earth Tech, Inc. Concord, MA*, *10*.
41. Sigmundsson, F., Einarsson, P., Hjartardóttir, Á. R., Drouin, V., Jónsdóttir, K., Arnadottir, T., Geirsson, H., Hreinsdottir, S., Li, S., & Ofeigsson, B. G. (2020). Geodynamics of Iceland and the signatures of plate spreading. *Journal of Volcanology and Geothermal Research*, *391*, 106436.
42. Sigmundsson, F., Hooper, A., Hreinsdóttir, S., Vogfjörd, K. S., Ófeigsson, B. G., Heimisson, E. R., Dumont, S., Parks, M., Spaans, K., & Gudmundsson, G. B. (2015). Segmented lateral dyke growth in a rifting event at Bárðarbunga volcanic system, Iceland. *Nature*, *517*(7533), 191–195.
43. Sigmundsson, F., Parks, M. M., Hooper, A., Geirsson, H., Vogfjörd, K., Drouin, V., Ófeigsson, B. G., Hreinsdóttir, S., Hjaltadóttir, S., Jónsdóttir, K., Einarsson, P., Barsotti, S., Horálek, J., & Ágústsdóttir, T. (2022). *Deformation and seismicity decline preceding a rift zone eruption at Fagradalsfjall, Iceland.*
44. Statistics in Iceland. (2022). *Inhabitants*. https://www.statice.is/statistics/population/inhabitants/
45. Sturkell, E., Einarsson, P., Sigmundsson, F., Geirsson, H., Olafsson, H., Pedersen, R., de Zeeuw-van Dalfsen, E., Linde, A. T., Sacks, S. I., & Stefánsson, R. (2006). Volcano geodesy and magma dynamics in Iceland. *Journal of Volcanology and Geothermal Research*, *150*(1–3), 14–34.
46. Sturkell, E., Sigmundsson, F., Einarsson, P., & Bilham, R. (1994). Strain accumulation 1986–1992 across the Reykjanes Peninsula plate boundary, Iceland, determined from GPS measurements. *Geophysical Research Letters*, *21*(2), 125–128.
47. Tarquini, S., de'Michieli Vitturi, M., Jensen, E. H., Pedersen, G. B., Barsotti, S., Coppola, D., & Pfeffer, M. A. (2018). *Modeling lava flow propagation over a flat landscape by using MrLavaLoba: The case of the 2014–2015 eruption at Holuhraun, Iceland*.
48. Vitturi, M. de'Michieli, & Tarquini, S. (2018). MrLavaLoba: A new probabilistic model for the simulation of lava flows as a settling process. *Journal of Volcanology and Geothermal Research*, *349*, 323–334.
49. Whitty, R. C., Ilyinskaya, E., Barsotti, S., Pfeffer, M. A., Roberts, T., Schmidt, A., Jóhannsson, Th., Gilbert, G., Hjörvar, T., Þrastarson, R., Fecht, D., Sigurðsson, E., & Sæmundsson, G. (in preparation). *SO2 and PM air quality and Icelandic population exposure during the 2021 Fagradalsfjall eruption*.

Figures

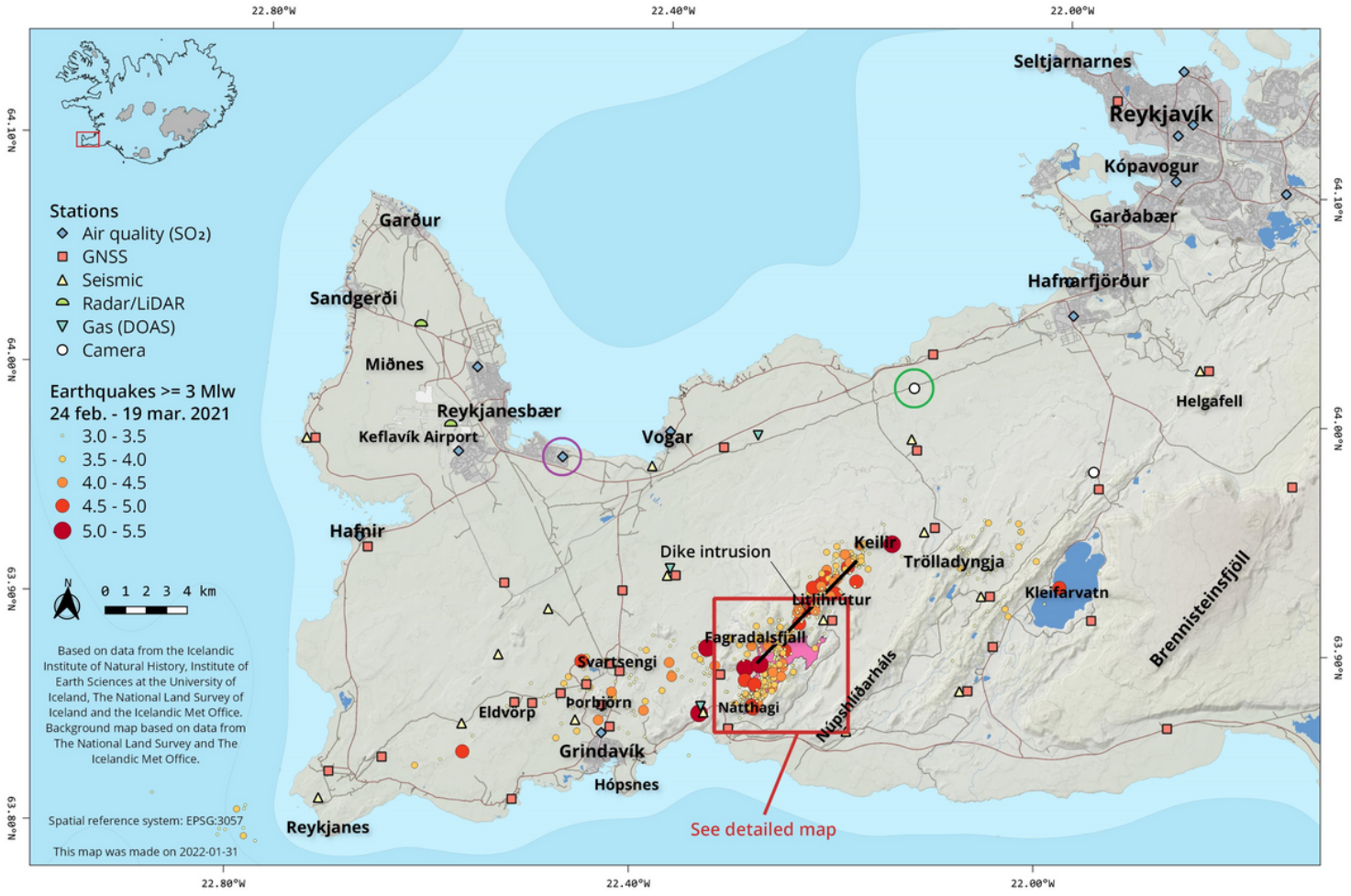

Figure 1

The Reykjanes Peninsula, the location of earthquakes above M3 for the period 24.02-19.03 2021 (colored filled circles), the dyke intrusion as mapped by InSAR images (black line) and location of Fagradalsfjall eruption site (plus the extension of lava field on 30 September 2021 as pink, see Figure 2). Monitoring stations are shown with different. Key sites mentioned in the text are also included.

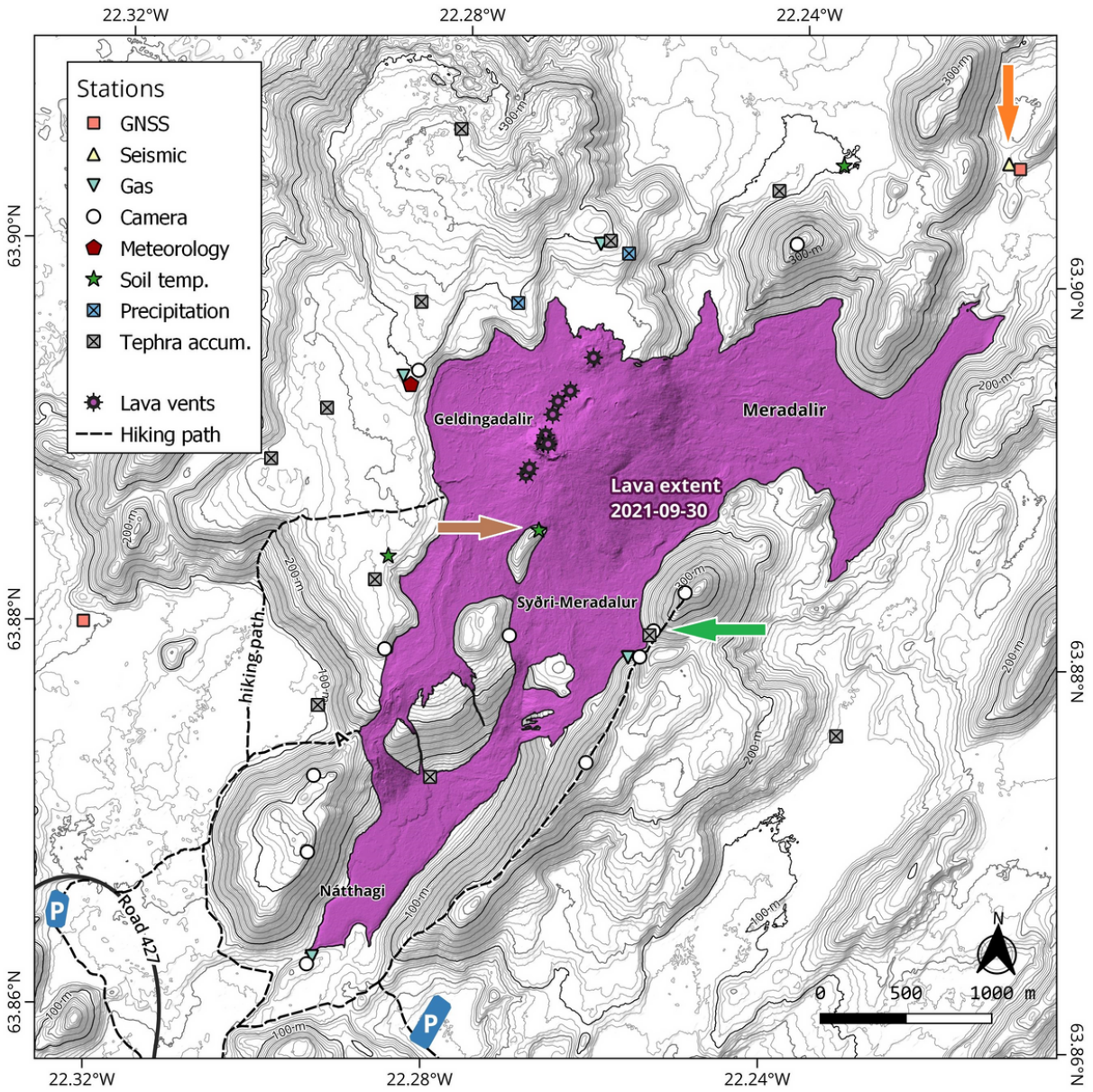

Figure 2

A detailed map of the eruption site showing the location of monitoring instrumentation around the eruption site (different stations are marked with different symbols). The final extension of the lava field at the end of the eruption is mapped in purple (survey performed on 30 September 2021 (G. B. M. Pedersen et al., 2021)*. Footpath and hiking trails are indicated as dashed lines, and two of the parking lots are showed and marked with P. The nine lava vents are showed as stars.*

Figure 3

(a) The large number of visitors formed a continuous line along the walking path to the eruption site. Photo taken on 24 March 2021; (b) People enjoying the view from the lower western slopes of Geldingadalir on 28 March 2021 (photos by B. Oddsson). In the months that followed both locations were covered with lava.

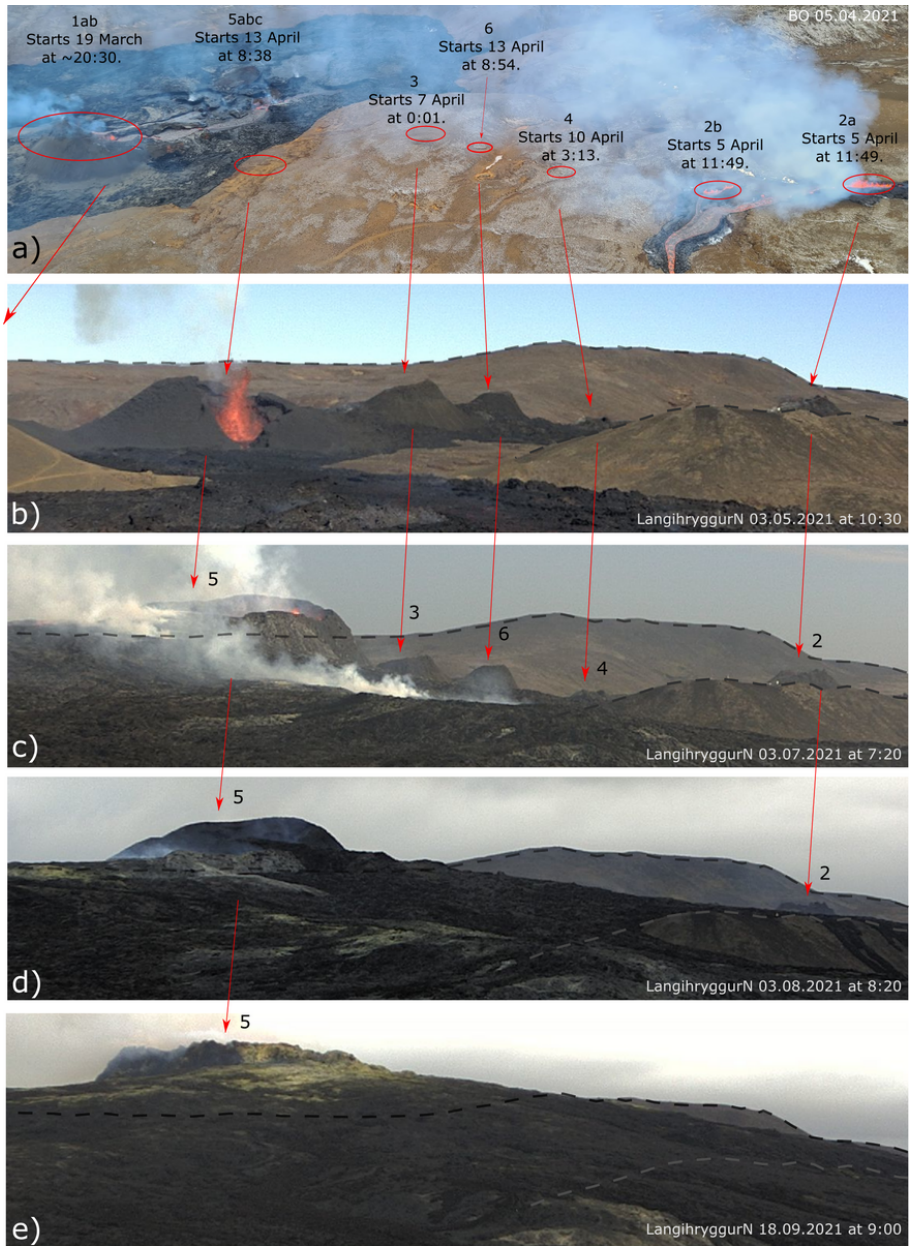

Figure 4

a) *Locations of eruptive openings and their timing, superimposed on a photo taken from the air on 5 April 2021; Evolution of the main crater (N. 5) b) 03 May, c) 03 July, d) 3 August and e) 18 September. Photos from a webcam located on Langihryggur, 1.4 km to the southeast of the main crater (Fig. 2 – green arrow). Note how the increasing height of the lava gradually obscures the viewto the opeinings active in April.*

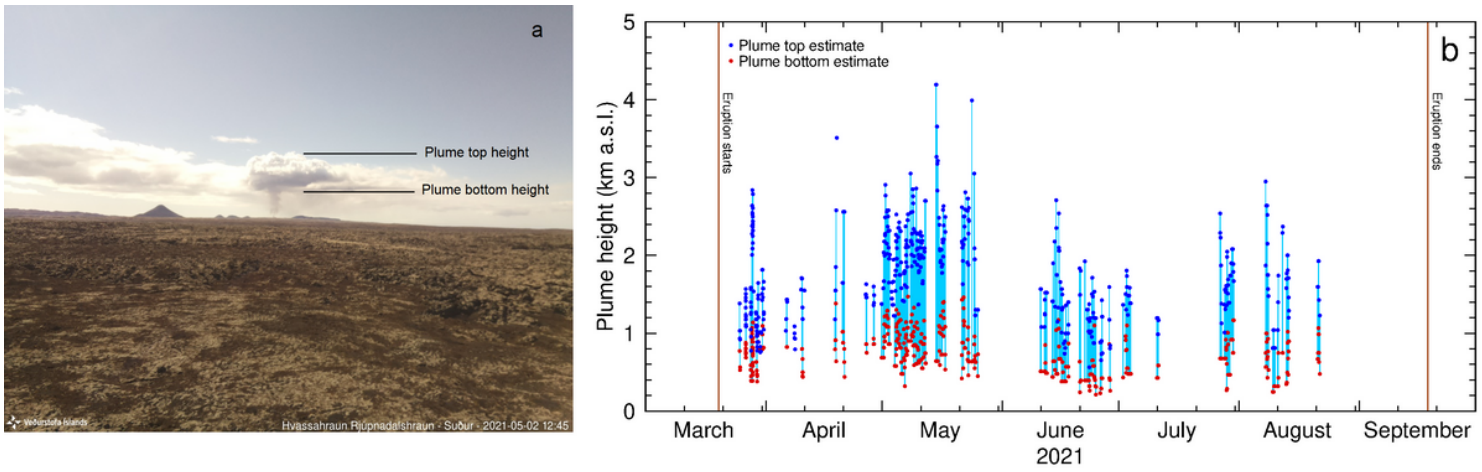

Figure 6

(a) The volcanic plume from Fagradalsfjall eruption on 2 May 2021 as seen from the Hvassahraun camera (see Fig. 1 – green circle); (b) The plume height as function of time as observed from the Hvassahraun camera for the period 25 March - 21 August 2021.

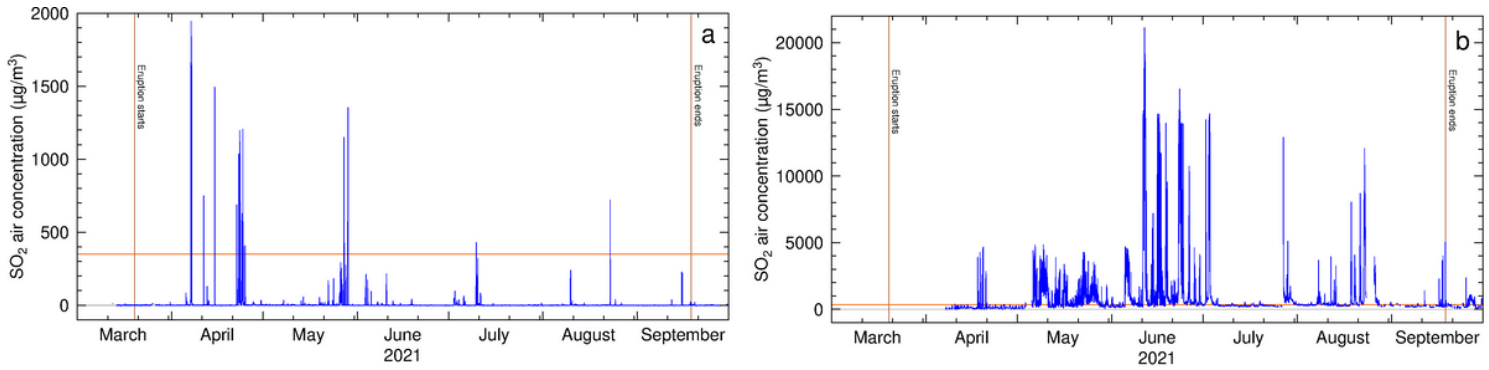

Figure 7

(a) Temporal evolution of SO_2 concentration at the station in Njarðvík (about 14 km NW of the eruption site – purple circle in Fig.2); (b) the SO_2 temporal evolution at one of the stations in closer proximity to the eruption site (about 550 m S of the main crater – brown arrow in Fig.2). Both plots show the concentration for the entire eruption period.

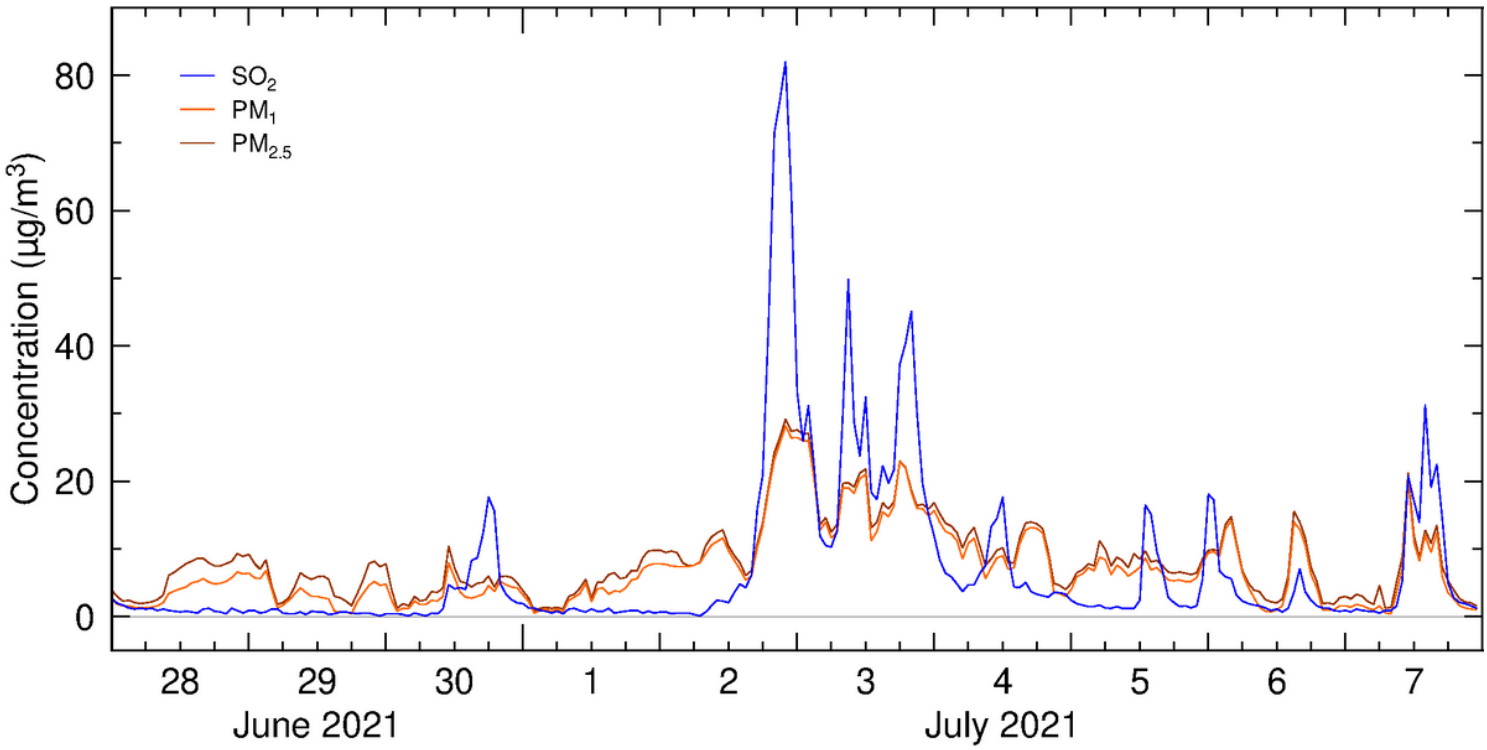

Figure 8

Temporal evolution of SO_2 and PM (2.5 and 1) at the Bústaðavegur station in Reykjavík (Fig. 1 for location) for the period 28 June - 7 July showing the temporal correlation between the different species which confirms the presence of volcanic sulphate in the plume reaching the Capital area.

Figure 9

Pumice grains produced during the Fagradalsfjall eruption (a) Pumice on the valley slopes about 600 m NNW of the Geldingadalir craters on 24 March 2021 during phase I of the eruption. (b) Pumice from the Fagradalsfjall eruption, collected on 24 March 2021. Longest axes of grains is up to 2.8 cm, most grains were < 1 cm in diameter (see a). c) Pumice in Nátthagi, about 2.5 km SSW of active vent, produced in May 2021 during phase V of the eruption. d) Pumice from Nátthagi 2.5 km SSW of crater. Longest axes of grains is up to 6.2 cm, collected on 19 May 2021. Photos: Bergrún Arna Óladóttir.

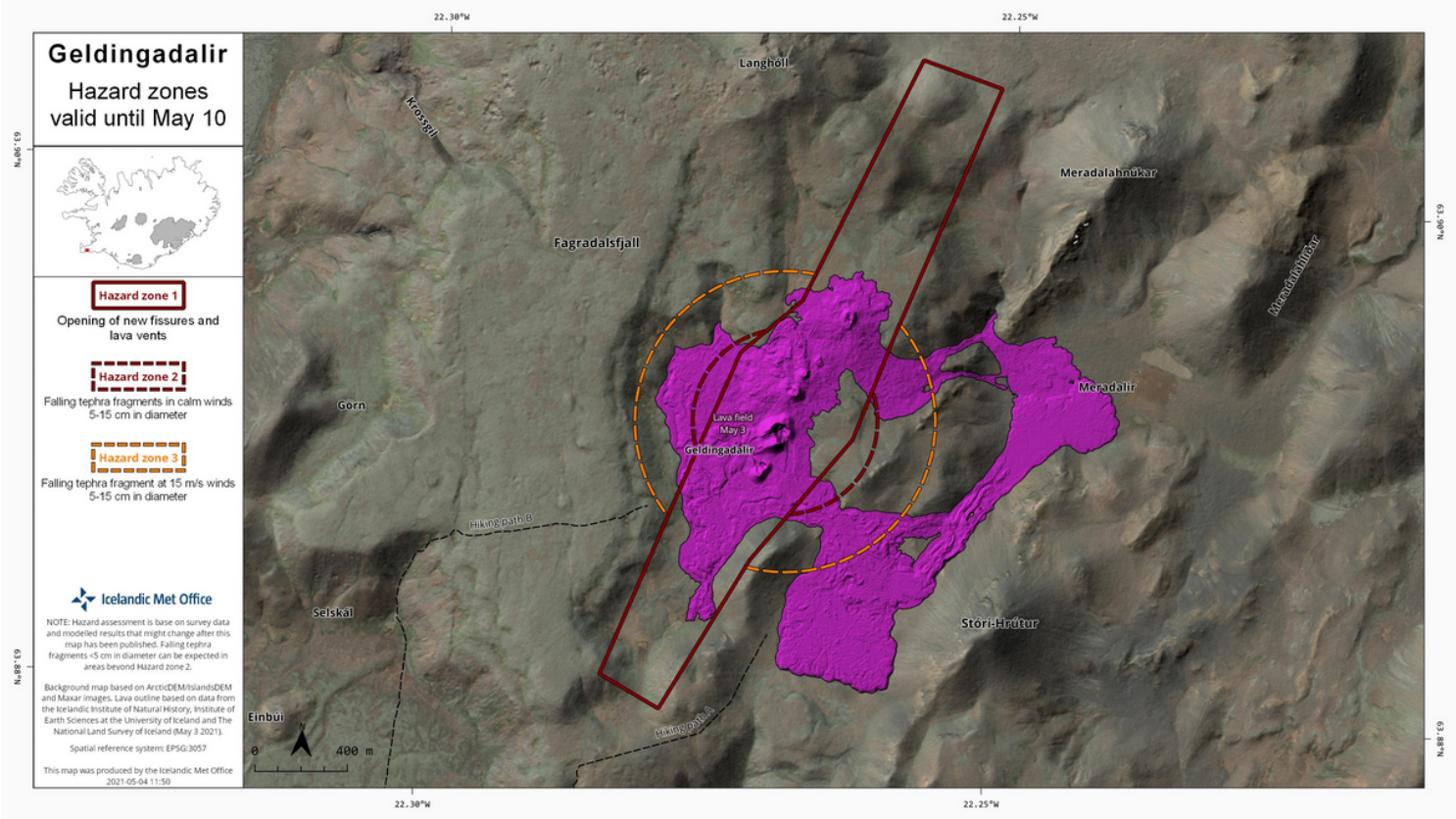

Figure 10

Hazard map that was prepared in May 2021, indicating the area where new accounting for the possible fissure openings were considered possible opening (red polygon) and area where fallout of large clasts from lava fountaining could happen (orange and red circles). The extent of the lava field at the time of making was also reported for reference. The map was adopted by Civil Protection and local Police for controlling and managing accesses to the eruption site.

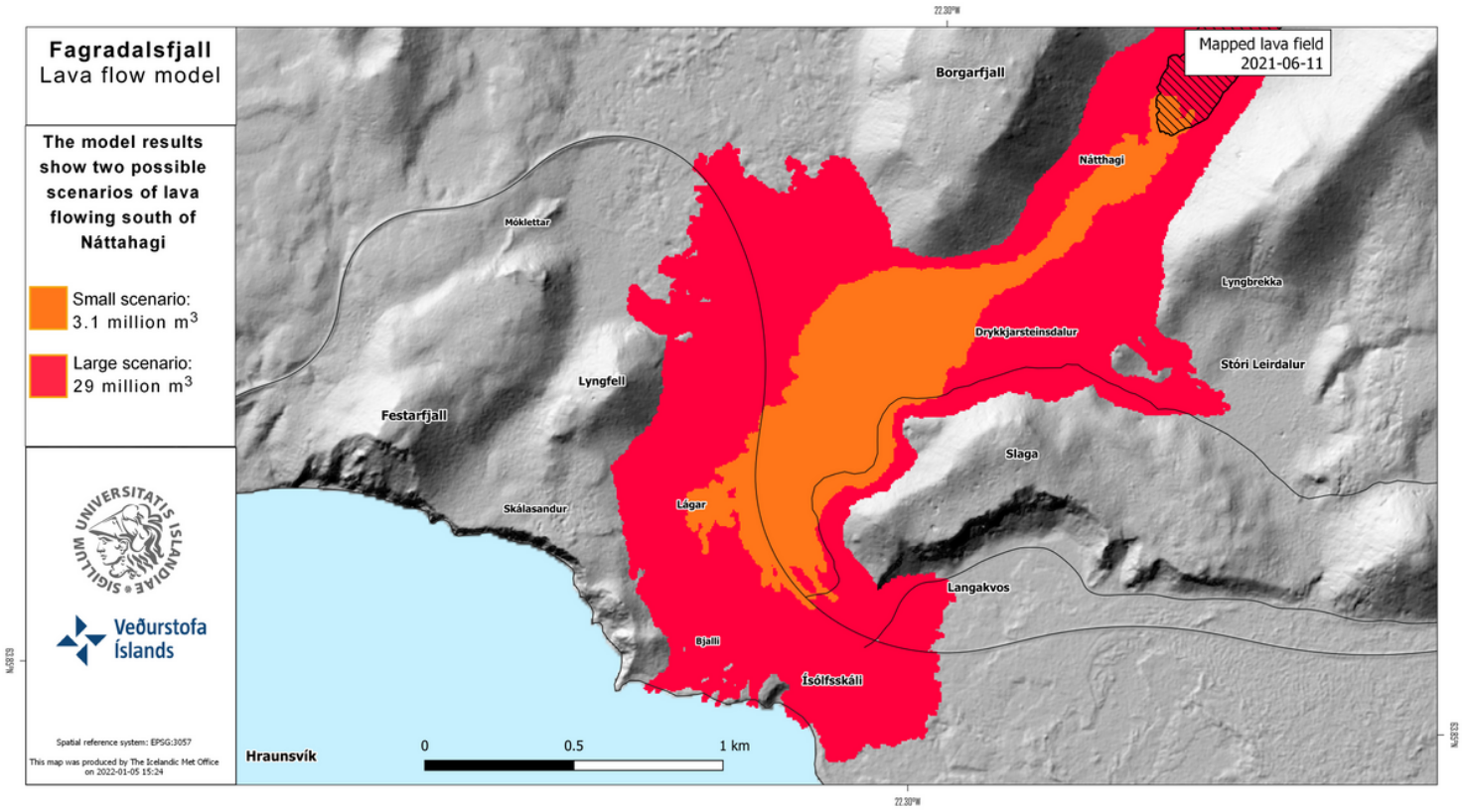

Figure 11

MrLavaLoba mModel results for two scenarios of lava flowing out of Nátthagi valley and reaching the coastline obtained from runs of MrLavaLoba. The map was published on the IMO's web site on the 22.06.2021. The two scenarios account for two different volumes of lava released at the edge of the lava field emplaced on the 11.06.2021: 3.1 m3 (orange area) and 29 m3 (red area), respectively.